J. Math. Anal. Appl. 563 (2026) 130801

Contents lists available at ScienceDirect

Journal of Mathematical Analysis and Applications

journal homepage: www.elsevier.com/locate/jmaa

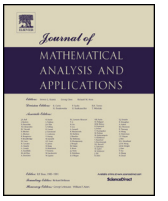

Regular Articles

Shortest paths in planar domains with hyperbolic type metrics ☆

Shuliang Gao [a,b], Anni Hakanen [c,d], Antti Rasila [a,b,*], Matti Vuorinen [d]

[a] *Department of Mathematics with Computer Science, Guangdong Technion - Israel Institute of Technology, 241 Daxue Road, Jinping District, Shantou, Guangdong 515063, People's Republic of China*
[b] *Department of Mathematics, Technion - Israel Institute of Technology, Haifa 32000, Israel*
[c] *Turku Collegium for Science, Medicine and Technology (TCSMT), University of Turku, Finland*
[d] *Department of Mathematics and Statistics, University of Turku, Finland*

ARTICLE INFO

Article history:
Received 24 January 2026
Available online 22 May 2026
Submitted by S. Hencl

Keywords:
Hyperbolic metric
Quasihyperbolic metric
Geodesic
Discrete conformal geometry
Geometric function theory
Dijkstra's algorithm

ABSTRACT

We study planar domains G equipped with a hyperbolic type metric and approximate geodesics that join two points $x, y \in G$ and their lengths. We present an algorithm that enables one to approximate the shortest distance in polygonal domains taken with respect to the quasihyperbolic metric. The method is based on Dijkstra's algorithm, and we give several examples demonstrating how the algorithm works and analyze its accuracy. We experimentally demonstrate several previously theoretically observed features of geodesics, such as the relationship between hyperbolic and quasihyperbolic distance in the unit disk. We also investigate bifurcation of geodesics and the connection of this phenomenon to the medial axis of the domain.

1. Introduction

The problem of finding a shortest path between two given locations is a classical problem in geodesy (see e.g. [32, Section 13.6]), and it has many connections to real world questions such as route planning, logistics, robotics, aviation, engineering, and communication networks. In this paper, we investigate this problem for hyperbolic type weighted metrics in planar domains (see [17]). One of the methods to study these problems is to discretize the underlying mathematical model by using graphs. The vertices of the graph are possible intermediate locations between initial and terminal locations, whereas the edges depict all the connections between vertices. The research literature of this part of mathematical graph theory is vast due to the possible savings as a result of process speedup of algorithms.

☆ Matlab source code for this paper is available from: https://github.com/arasila/quasihyperbolic_geodesics.

* Corresponding author at: Department of Mathematics with Computer Science, Guangdong Technion, 241 Daxue Road, Jinping District, Shantou, Guangdong 515063, People's Republic of China.

E-mail addresses: gao09228@gtiit.edu.cn (S. Gao), anehak@utu.fi (A. Hakanen), antti.rasila@iki.fi, antti.rasila@gtiit.edu.cn (A. Rasila), vuorinen@utu.fi (M. Vuorinen).

https://doi.org/10.1016/j.jmaa.2026.130801

We study this shortest path problem in a planar domain with a given metric with some special features: in particular, this metric measures not only the distance between two points but also their location with respect to the boundary of the domain. In the cases we study, the existence of shortest paths between two given points, i.e. length-minimizing curves or geodesics, is known by theory. A characteristic feature of the geodesics of hyperbolic type metrics is that they have a tendency to avoid the boundary of the domain as much as possible.

1.1. Weighted metrics

For a domain $G \subsetneq \mathbb{R}^n, n \geq 2$, define a continuous function $w : G \to (0, \infty)$, called *weight function* and the *weighted length* of a rectifiable curve γ in G by

$$\ell_G^w(\gamma) = \int_\gamma w(z)\,|dz|\,. \tag{1.1}$$

If $w(x) = 1$ for all $x \in G$, then $\ell_G^w(\gamma)$ reduces to the Euclidean length of γ, and if

$$w(z) = \frac{1}{d(z, \partial G)}\,, \tag{1.2}$$

where $d(z, \partial G)$ is the distance of $z \in G$ from the boundary of the domain, then $\ell_G^w(\gamma)$ is the *quasihyperbolic length* of γ. The quasihyperbolic distance is defined for $x, y \in G$ as

$$k_G(x, y) = \inf_\gamma \int_\gamma \frac{|dz|}{d(z, \partial G)}\,, \tag{1.3}$$

where the infimum is taken over all rectifiable curves γ in G with $x, y \in \gamma$. This metric was defined by F.W. Gehring and his coauthors B.P. Palka [16] and B. Osgood [15], who also studied its applications in geometric function theory. In particular, they showed that the distance function (1.3) defines a metric and that there exists a length minimizing curve, geodesic, joining the points x and y. Interestingly, this is not necessarily true in more general settings like Banach spaces (see [30]).

Since its introduction, the quasihyperbolic metric has become a standard tool in the study of geometric function theory, quasiconformal mappings, and analysis on metric spaces [13,14,17,20,31], where it is typically used as the substitute for hyperbolic metric in the cases where hyperbolic metrics cannot be defined. For half-planes and half-spaces, the quasihyperbolic metric coincides with the hyperbolic metric, and when the domain G is a simply connected domain of the plane, it differs from the hyperbolic metric [3] at most by a constant factor [13]. This serves as a motivation for the Gromov hyperbolic uniformization theory, introduced by Bonk, Heinonen, and Koskela in the seminal paper [5], where the question of Gromov hyperbolicity of quasihyperbolic metrics plays a central role. As far as we know, the algorithm given in this paper is the first general method for approximation of geodesics and distances in quasihyperbolic metric.

1.4. Approximation of quasihyperbolic geodesics. In spite of all these applications, finding the explicit value of the quasihyperbolic distance is not possible except in a few special cases. Therefore, during the past five decades many comparison metrics have been introduced that are easily evaluated and, at the same time, give either upper or lower bounds for the quasihyperbolic metric. For a survey of these comparison metrics, see [17] and the recent article [27].

In this study, quasihyperbolic geometry is investigated from the point of view of constructive approximation. We discretize the problem by forming a grid of points in the domain G. This grid must be fine enough considering the mutual locations of the points and the geometric features of the domain G. We define a graph using these grid points and define the distance between two neighboring points in a manner that is compatible with the quasihyperbolic geometry. The main step of the process is to find the shortest path in this graph. For this purpose we use Dijkstra's algorithm [7]. This method applies not only for the quasihyperbolic metric but also for many other weighted metrics for which shortest paths joining the points are known to exist. The method enables us to approximate the quasihyperbolic geodesics by means of polygonal curves and present figures of these approximations in several polygonal domains. We also compare our approximate values of the quasihyperbolic distances to approximations obtained by other methods.

After this introduction the contents of this paper is organized as follows. In Section 2 we introduce some basic notation for the metrics we use, describe how to proceed from grid points of a domain to a graph, and some facts about special functions. In Section 3 we discuss computing distances in graphs and introduce Dijkstra's algorithm and discuss implementation of the algorithm for approximation of geodesics based on Dijkstra's algorithm. In Section 4 we use this algorithm for approximation of hyperbolic and quasihyperbolic geodesics in the unit disk, with an aim of validating the method and understanding its accuracy. We also consider conformal mappings of the upper half-plane onto two polygonal domains, expressed in terms of Schwarz-Christoffel integrals. In Section 5 we investigate cases where non-uniqueness and bifurcation of geodesics is expected from theoretical considerations. In Sections 6–8 we consider other interesting examples where hyperbolic and quasihyperbolic geodesics can be approximated by using our methods. Finally, in Section 9, we give our final conclusions.

2. Preliminaries

In this section, we give the formulas and results needed later in our examples. We first focus on hyperbolic geometry and then present the necessary tools in order to handle conformal mappings of the upper half-plane onto a quadrilateral domain.

2.1. Hyperbolic geometry. We recall some basic formulas and notation for hyperbolic geometry from [3]. The hyperbolic metrics of the unit disk $\mathbb{B}^2$ and the upper half-plane $\mathbb{H}^2$ are defined, respectively, by

$$\sinh\left(\frac{\rho_{\mathbb{B}^2}(a,b)}{2}\right) = \frac{|a-b|}{\sqrt{(1-|a|^2)(1-|b|^2)}}, \quad a,b \in \mathbb{B}^2, \tag{2.2}$$

and

$$\cosh\left(\rho_{\mathbb{H}^2}(x,y)\right) = 1 + \frac{|x-y|^2}{2\mathrm{Im}(x)\mathrm{Im}(y)}, \quad x,y \in \mathbb{H}^2. \tag{2.3}$$

By the Riemann mapping theorem, one can map a simply connected planar domain D, not equal to the whole plane, onto the unit disk by means of a conformal mapping $f : D \to \mathbb{B}^2$ and define the hyperbolic metric for $a, b \in D$ as follows

$$\rho_D(a,b) = \rho_{\mathbb{B}^2}(f(a), f(b)).$$

This definition is possible due to the *conformal invariance* of the hyperbolic metric [22].

Numerical methods to find the hyperbolic distance between two given points in a simply connected planar domain and to draw the hyperbolic geodesic joining the points are given in [29].

2.4. Distance ratio metric. A useful comparison metric for the quasihyperbolic metric is the distance ratio metric [16]

$$j_G(x,y) = \log\left(1 + \frac{|x-y|}{\min\{d(x,\partial G), d(y,\partial G)\}}\right), \tag{2.5}$$

where $x, y \in G$. The metrics j_G and k_G are not conformally invariant, and they are only similarity invariant. If $G \in \{\mathbb{B}^2, \mathbb{H}^2\}$, then for $x, y \in G$

$$j_G(x,y) \le \rho_G(x,y) \le 2j_G(x,y), \tag{2.6}$$

$$k_G(x,y) \le \rho_G(x,y) \le 2k_G(x,y). \tag{2.7}$$

In fact, $k_G \equiv \rho_G$ for $G = \mathbb{H}^2$. The geodesics of the quasihyperbolic metric are smooth [25].

For all domains G, we have a simple lower bound for the quasihyperbolic metric

$$k_G(x,y) \ge j_G(x,y) \ge \left|\log \frac{d(x,\partial G)}{d(y,\partial G)}\right|. \tag{2.8}$$

In view of the above two-sided inequalities (2.6) and (2.7) and the lower bound (2.8) it is natural to ask for which classes of domains there is a majorant for k_G in terms of j_G. Indeed, inequalities between metrics can be used to define some important classes of domains. Thus, for instance, the class of simply connected plane domains G for which there exists a constant $A \ge 1$ such that for all $x, y \in G$

$$k_G(x,y) \le A\, j_G(x,y) \tag{2.9}$$

defines the class of quasidisks studied in [13]. Domains of this class, in turn, are special cases of the so called φ-uniform domains [17].

2.10. The medial axis. The medial axis of a planar domain is the set of all those points of the domain that have at least two closest boundary points. Thus, for a sector with angle $\theta \in (0, \pi)$, the angle bisector is the medial axis. For an ellipse domain, a part of the major axis is the medial axis.

Lindén showed in his PhD thesis [24] that if two points of a convex sector are far enough from each other, then the quasihyperbolic geodesic joining them consists of three pieces linked together. Two pieces are sub-arcs of circles, each circle orthogonal to a side of the sector and tangential to the sector bisector at a contact point, whereas the third piece is the subsegment of the bisector joining these two contact points. See also Hästö [18].

2.11. Approximation of the weighted length of a polygonal curve. Let $x_j, j = 1, \ldots, p$, be points in a domain $G \subset \mathbb{R}^n$ and consider the polygonal curve $\gamma = \cup_{j=1}^{p-1} [x_j, x_{j+1}]$. For a given weight function $w : G \to (0, \infty)$ we can approximate $\ell_G^w(\gamma)$ provided that $\gamma \subset G$ which clearly holds if G is convex or, more generally, if all the segments $[x_j, x_{j+1}] \subset G, j = 1, \ldots, p-1$. In what follows we assume that this last condition is fulfilled.

From the definition (1.3) of the quasihyperbolic metric it is clear that a simple approximation is

$$\ell_G^w(\gamma) \approx \sum_{j=1}^{p-1} w_j |x_j - x_{j+1}| \tag{2.12}$$

where the coefficient w_j depends on the weight function w. It is a natural requirement that w_j depends on the points x_j and x_{j+1} in a symmetric manner, because $\ell_G^w(x_j, x_{j+1}) = \ell_G^w(x_{j+1}, x_j)$. Therefore we can choose e.g.

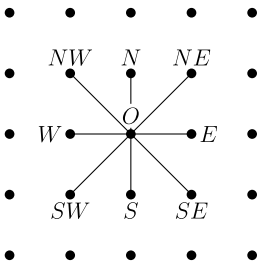

Fig. 1. A grid point O with a maximal number, eight, neighboring points as described in 2.15 (without a refinement of the grid).

$$w_j = \frac{1}{\min\{d(x_j, \partial G), d(x_{j+1}, \partial G)\}} \tag{2.13}$$

in the case of the quasihyperbolic metric; this is what we use in the experiments reported below.

The case of a general weight function is more difficult because the oscillation of the function w is uncontrolled. For the purpose of controlling the oscillation of the function w one could require that w satisfies a Harnack inequality: there exist constants $\lambda \in (0,1)$ and $C_\lambda \geq 1$ such that

$$\max_{B_x} w(z) \leq C_\lambda \min_{B_x} w(z) \tag{2.14}$$

holds for all $B^n(x,r) \subset G$ where $B_x = \overline{B}^n(x, \lambda r)$. If it is true that, for the above polygon and for all $j = 1, \ldots, p-1$,

$$[x_j, x_{j+1}] \subset B^n(x_j, \lambda d(x_j))$$

and the Harnack condition holds, then we could estimate the error in the approximation (2.12). Note that the quasihyperbolic weight function $1/d(x, \partial G)$ satisfies the above Harnack condition.

2.15. Grid points. For the purpose of approximating distances between point pairs in a planar domain G, we generate, for a given mesh size $h > 0$, a grid of those points of the Cartesian lattice $h\mathbb{Z}^2$, which are in the domain G.

Then for each grid point we define its set of neighboring points. We use the geographical directions to label these, the four cardinal directions – north (N), east (E), south (S), and west (W) – and the four intermediate directions – northeast (NE), southeast (SE), southwest (SW), and northwest (NW), see Fig. 1. The set of neighboring points of a grid point x may either be empty or contain p points, $1 \leq p \leq 8$, depending on $d(x, \partial D)$ and the mesh size h. Observe that if x is a neighbor of y then also y is a neighbor of x.

2.16. From a grid to a graph. We now set up a graph using the grid points of a domain G constructed above as vertices of a graph and defining the distance $d(x,y)$ between two neighboring points x and y such that $d(x,y) = d(y,x)$. In what follows, d is usually a weighted metric, in most cases the quasihyperbolic metric. For the purpose of approximating the shortest path between two grid points x and y, we will apply Dijkstra's algorithm. For our method to work, there must exist at least one polygonal curve $\cup_{j=1}^{k-1}[p_j, p_{j+1}]$, with $p_1 = x$ and $p_k = y$ such that p_{j+1} is a neighbor of p_j and $[p_j, p_{j+1}] \subset G$, for each $j = 1, \ldots, k-1$. It is easily seen that this last condition is satisfied if $d(p_j, \partial G) \geq 2h$, for all $j = 1, \ldots, k$. Dijkstra's algorithm provides a simple and robust method for finding the shortest distance between two points of the graph.

2.17. From a graph to an algorithm. The above method can be improved by refining the grid. We now describe the details of this refinement idea. Indeed, we increase the number of neighboring points by accepting

certain points of the refined grid $G \cap \frac{h}{m}\mathbb{Z}^2$ where $m \in \mathbb{N}$, as neighbors of a given point x in the original grid. This expanded set of neighbors is defined for a positive parameter $m \in \mathbb{N}$ as follows:

$$N_x = \{p \in G \cap \frac{h}{m}\mathbb{Z}^2 \mid h \cdot m \leq |p - x| \leq \sqrt{2} \cdot h \cdot m\}. \tag{2.18}$$

Fig. 2 illustrates the set N_x for different values of m. Observe that if N_x contains y, then also N_y contains x. This expansion of neighboring points means that the cardinality of the set N_x depends on m and can, in particular, be larger than 8. We have not fixed the parameter m uniformly in this paper and plan to study in our future research the influence of m on the accuracy of the computation.

We now set up a graph using the grid points of a domain G constructed above as vertices of a graph by using the method mentioned above to construct N_x and to approximate the distance $d(x, y)$ between two neighboring points x and $y \in N_x$ such that $d(x, y) = d(y, x)$. In what follows, d is a weighted metric, in most cases the quasihyperbolic metric.

We will apply Dijkstra's algorithm to approximate the shortest path between two grid points x and y. For this method to work, there must exist at least one polygonal curve $\cup_{j=1}^{k-1}[p_j, p_{j+1}]$, $p_j, j = 1, \ldots, k$, with $p_1 = x$ and $p_k = y$ such that p_{j+1} is a neighbor of p_j and $[p_j, p_{j+1}] \subset G$, for each $j = 1, \ldots, k-1$. It is easily seen that this last condition is satisfied if $d(p_j, \partial G) \geq 2h$, for all $j = 1, \ldots, k$. Our algorithm is described in detail in Section 3.

2.19. Special functions. Conformal mappings expressed in terms of special functions are frequently used in study of conformal invariants. In this paper, we apply the Schwarz-Christoffel formula which gives a conformal mapping of the upper half-plane onto a polygon in terms of an integral. This formula is useful in the case where the polygon is a quadrilateral and the conformal mapping is given by a hypergeometric function.

Let Γ denote Euler's *gamma function* $\Gamma(z)$ and $B(a, b)$ the beta function

$$B(a, b) = \frac{\Gamma(a)\Gamma(b)}{\Gamma(a + b)}.$$

Given complex numbers a, b, and c with $c \neq 0, -1, -2, \ldots$, the *Gaussian hypergeometric function* is the analytic continuation to the slit plane $\mathbb{C} \setminus [1, \infty)$ of the series

$$F(a, b; c; z) = {}_2F_1(a, b; c; z) = \sum_{n=0}^{\infty} \frac{(a, n)(b, n)}{(c, n)} \frac{z^n}{n!}, \quad |z| < 1\,. \tag{2.20}$$

Here $(a, 0) = 1$ for $a \neq 0$, and (a, n) is the *shifted factorial function* or the *Appell symbol*

$$(a, n) = a(a + 1)(a + 2) \cdots (a + n - 1)$$

for $n \in \mathbb{N} \setminus \{0\}$, where $\mathbb{N} = \{0, 1, 2, \ldots\}$. Denote $C = C(b, c) = 1/B(b, c - b)$. We define the function f given on the closed upper half-plane by

$$w = f(z) = f_{a,b,c}(z) = C \int_0^z g_r(t)dt \tag{2.21}$$

$$= C \int_0^z t^{b-1}(1 - t)^{c-b-1}(1 - r^2 t)^{-a} dt \tag{2.22}$$

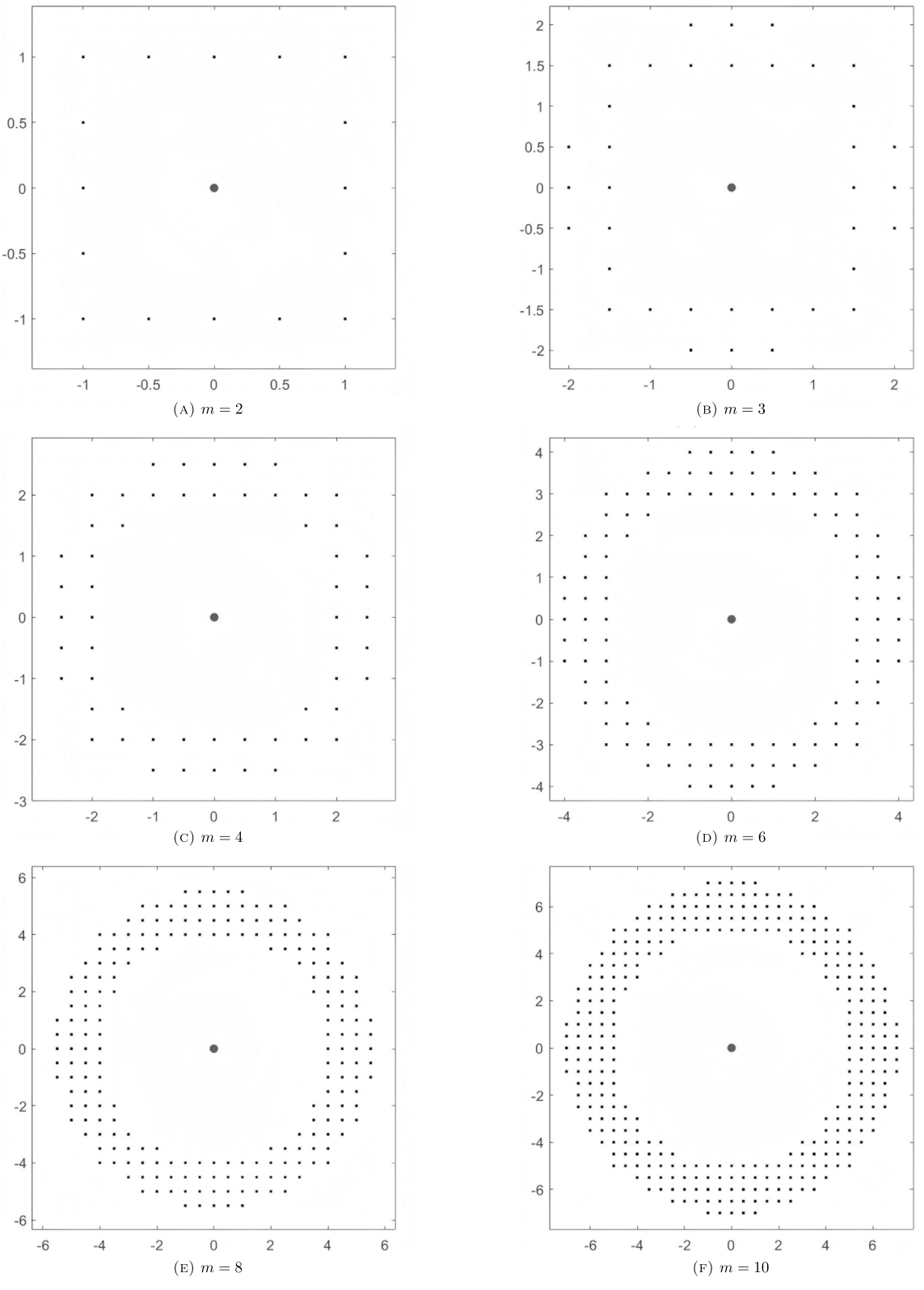

(A) $m = 2$ (B) $m = 3$

(C) $m = 4$ (D) $m = 6$

(E) $m = 8$ (F) $m = 10$

Fig. 2. The m-neighborhoods of origin point $x = 0$ with $h = 0.5$.

$$= e^{i(a+b+1-c)\pi} C r^{-2a} \int_0^z t^{b-1}(t-1)^{c-b-1}(t-1/r^2)^{(1-a)-1} dt\,. \tag{2.23}$$

Recall the Euler integral representation [2, Theorem 2.2.1] and [1, 15.3.1]

$$F(a,b;c;z) = \frac{\Gamma(c)}{\Gamma(b)\Gamma(c-b)} \int_0^1 t^{b-1}(1-t)^{c-b-1}(1-tz)^{-a} dt \tag{2.24}$$

$$= C(b,c) e^{i(a+b+1-c)\pi} \int_0^1 t^{b-1}(t-1)^{c-b-1}(tz-1)^{-a} dt$$

for $\mathrm{Re}(c) > \mathrm{Re}(b) > 0$ and $z \in \mathbb{C} \setminus \{u \in \mathbb{R} \mid u \geq 1\}$.

Theorem 2.25. *[19, Theorem 2.4] Let H denote the closed upper half-plane $\{z \in \mathbb{C} \mid \mathrm{Im}\,(z) \geq 0\}$ and let $0 < a, b < 1, \max\{a+b, 1\} \leq c \leq 1+\min\{a,b\}$, $r \in (0,1)$. Then the function f in (2.22) is a homeomorphism of H onto the quadrilateral Q with vertices*

$$f(0) = 0\,,\ \ f(1) = F(a,b;c;r^2)\,,$$
$$f(1/r^2) = f(1) + \frac{B(c-b,1-a)}{B(b,c-b)} e^{(b+1-c)i\pi} (1-r^2)^{2(c-a-b)} F(c-a,c-b;c+1-a-b;(1-r^2)^2)\,,$$

and

$$f(\infty) = f(1/r^2) + \frac{B(1-a,a+1-c)}{B(b,c-b)} e^{i(a+b+1-c)\pi} r^{2(1-c)} r'^{2(c-a-b)} F(1-b,1-a;2-c;r^2)\,,$$

and interior angles $b\pi, (c-b)\pi, (1-a)\pi$ and $(a+1-c)\pi$, respectively, at these vertices. It is conformal in the interior of H.

3. Dijkstra's algorithm and approximation of geodesics

3.1. Graphs and paths. A *digraph* consists of vertices that are connected to each other by arcs. Formally, the vertex set of a digraph D is denoted by $V(D)$ and the arc set by $A(D)$. The arc set $A(D)$ consists of ordered pairs (u,v) where $u, v \in V(D)$. An undirected graph is a special case of a digraph where $(u,v) \in A(D)$ if and only if $(v,u) \in A(D)$. Digraphs do not necessarily satisfy this bidirectionality of arcs. A *weighted digraph* is a digraph where each arc (u,v) is associated with a *weight* $w((u,v)) \in \mathbb{R}$.

A *path* from a vertex u_0 to another vertex u_k is a sequence of vertices $u_0u_1\cdots u_k$ where no vertex repeats and $(u_i, u_{i+1}) \in A(D)$ for all u_i. The distance from u to v (denoted by $\mathrm{dist}(u,v)$) is the minimum number of arcs along a path from u to v when the digraph is unweighted. If the digraph is weighted, the distance from u to v is defined as

$$\mathrm{dist}(u,v) = \min\left\{ \sum_{i=0}^{k} w((u_i,u_{i+1})) \,\middle|\, u_0,\ldots,u_k \text{ is a path from } u=u_0 \text{ to } v=u_k \right\}.$$

3.2. Dijkstra's algorithm. The distances in a weighted digraph with non-negative weights can be computed with Dijkstra's algorithm [7] which was introduced in 1959. This algorithm computes the distances from a single vertex u to all other vertices in D. At first, each vertex $v \in V(D)$ is given an estimate $d(v)$ of the distance from u to v. Initially, $d(u) = 0$ and $d(v) = \infty$ for all $v \in V(D) \setminus \{u\}$. Along the execution of the

algorithm, we mark vertices and initially all vertices are unmarked. The following step is repeated until all vertices are marked.

We choose the vertex x to be an unmarked vertex with $d(x)$ as small as possible ($x = u$ in the first iteration). For all v such that $(x, v) \in A(D)$, we update $d(v)$ to be $d(x) + w((x, v))$ if this is smaller than the current value of $d(v)$. Finally, we mark x and sort the unmarked vertices according to the current estimates.

When this step is iterated until all vertices are marked, the execution ends and we have $d(v) = \mathrm{dist}(u, v)$ for all $v \in V(D)$. The sorting of the vertices according to their distance estimates can be done using Fibonacci heaps [12]. Then the running time of the algorithm is $\mathcal{O}(m + n \log n)$, where $m = |A(D)|$ and $n = |V(D)|$.

3.3. Dijkstra's algorithm compared to other path finding methods. Despite its age and simplicity, Dijkstra's algorithm remains one of the fastest and most used algorithms of computing distances in weighted graphs. If negative edge weights are allowed (but there are no negative cycles), the distances can be computed using the Bellman-Ford-Moore algorithm [4,11,28]. If the digraph is unweighted, it is faster to use a simple algorithm adapted from breadth-first-search. During the preparation of this article, Duan et al. [10] showed that there exists an algorithm running in $\mathcal{O}(m \log^{2/3} n)$ time for computing the distances from one vertex to all others in a weighted digraph with non-negative edge weights. This is the long-awaited improvement to Dijkstra's algorithm, which has turned out difficult to improve due to the sorting step. However, Duan et al. make several assumptions to simplify the presentation of their algorithm. Most notably, the graphs are assumed to be sparse and every vertex has constant in- and out-degree. The algorithm they present is generalizable to graphs without these constraints. Dijkstra's algorithm is readily available and well-optimized for different programming languages, which is why we chose to use Dijkstra's algorithm and not to implement Duan et al.'s algorithm for the purposes of our experiments.

3.4. Implementation of an algorithm for approximation of geodesics. Due to practical concerns with the numerical approximation, we use a version of the conformal density function modified from the usual definitions of hyperbolic and quasihyperbolic densities.

3.5. Dijkstra's algorithm and weighted metrics. We first generate an undirected weighted graph $G^* = (V, E, W)$ with mesh size h, parameter m and definition of neighborhood points defined in (2.18), and then apply Dijkstra algorithm on G^*. The precise definition of the applied method is given as in Algorithm 1.

3.6. Remark. It should be noted that a straight-forward application of the above methods leads to low efficiency because in most cases it is enough to carry out the refinement in a subdomain instead of the whole domain. Therefore, it is better to generate the uniform mesh in the region around a^*, b^*, defining $x_{\min}, x_{\max}, y_{\min}, y_{\max}$ as below:

$$\begin{cases} x_{\min} := \min\{\mathrm{Re}\,(a^*), \mathrm{Re}\,(b^*)\} - k_{x_{\min}} \cdot h, \\ x_{\max} := \max\{\mathrm{Re}\,(a^*), \mathrm{Re}\,(b^*)\} + k_{x_{\max}} \cdot h, \\ y_{\min} := \min\{\mathrm{Im}\,(a^*), \mathrm{Im}\,(b^*)\} - k_{y_{\min}} \cdot h, \\ y_{\max} := \max\{\mathrm{Im}\,(a^*), \mathrm{Im}\,(b^*)\} + k_{y_{\max}} \cdot h, \end{cases}$$

where $k_{x_{\min}}, k_{y_{\min}}, k_{x_{\max}}, k_{y_{\max}}$ are set manually. Then we apply Algorithm 1 on the region $[x_{\min}, x_{\max}] \times [y_{\min}, y_{\max}] \cap G$ to generate the local approximated geodesic. We mainly apply this method in our following experiments, and call it applying Algorithm 1 locally.

Algorithm 1 Graph Construction and Shortest Path Approximation, [26]

Require: Region $G \subset [a,b] \times [c,d]$, mesh size h, layer parameter m, weight function w, start point p_1, end point p_2
Ensure: Undirected weighted graph $G^* = (V, E, W)$, shortest path γ^* between p_1 and p_2, shortest path's length ℓ

Part 1: Graph Construction
Step 1: Construct vertices V.
$V \leftarrow \emptyset$
for $j = 0$ **to** $\lfloor (b-a)/h \rfloor$ **do**
  for $k = 0$ **to** $\lfloor (d-c)/h \rfloor$ **do**
    $x \leftarrow a + j \cdot h \in \mathbb{R}$
    $y \leftarrow c + k \cdot h \in \mathbb{R}$
    $p \leftarrow x + y \cdot i \in \mathbb{C}$
    if $p \in G$ **then**
      $V \leftarrow V \cup \{p\}$
    end if
  end for
end for
Step 2: Construct edges E.
$E \leftarrow \emptyset$
for $p \in V$ **do**
  $\mathrm{Layer}_m(p) \leftarrow \{q \in V : m \cdot h \le \|p - q\| \le \sqrt{2} \cdot m \cdot h\}$
  for $p_i \in \mathrm{Layer}_m(p)$ **do**
    if Segment $[p, p_i]$ does not intersect with G **then**
      $E \leftarrow E \cup \{(p, p_i)\}$
    end if
  end for
end for
Step 3: Construct weights W:
$W \leftarrow \emptyset$
for $e \in E$ **do**
  $W \leftarrow W \cup \{w(e)\}$
end for
$G^* = (V, E, W)$
Part 2: Shortest Path Calculation
Step 1: Find the closest points to p_1, p_2 in V.
$\mathrm{idx1} \leftarrow \arg\min |zv - p_1|$
$\mathrm{idx2} \leftarrow \arg\min |zv - p_2|$
Step 2: Find shortest path and its length.
$[\gamma^*, \ell] \leftarrow$ **shortestpath**$(G^*, \mathrm{idx1}, \mathrm{idx2})$ {Dijkstra's algorithm returning both path and length [26]}
return G^*, γ^*, ℓ

3.7. Hyperbolic geodesics. Let $G \subset \mathbb{C}$ be a simply connected domain, and let $f : \mathbb{H}^2 \to G$ be a conformal mapping (implemented via Schwarz-Christoffel transformation). For any $a^*, b^* \in G$, the discretization of the hyperbolic geodesic $\gamma_{\rho_G}(a^*, b^*)$ on G is constructed as follows:

Let $a = f^{-1}(a^*)$, $b = f^{-1}(b^*)$. Then we know the hyperbolic geodesic $\gamma_{\rho_{\mathbb{H}^2}}(a, b)$ on $\mathbb{H}^2$. We choose a discrete set of points $\{z_i\}_{i=1}^n \subset \gamma_{\rho_{\mathbb{H}^2}}(a, b)$ satisfying:

$$z_1 = a, \quad z_n = b,$$
$$\|z_{i+1} - z_i\| = \Delta s, \quad i = 1, \ldots, n-1,$$

where Δs is the size of the discretization step. Then we obtain the point sequence on G via conformal mapping: $w_i = f(z_i)$, $i = 1, \ldots, n$. The final curve is defined as:

$$\gamma_{\rho_G}(a^*, b^*) = \{w_i\}_{i=1}^n.$$

3.8. Approximated hyperbolic geodesics. For any $a^*, b^* \in G$, the approximated hyperbolic geodesic $\gamma^*_{\rho_G}(a^*, b^*)$ on G is constructed via the following discrete approximation scheme: Let $a = f^{-1}(a^*)$, $b = f^{-1}(b^*)$. We define the distance between z_i and z_j as $\rho_{\mathbb{H}^2}(f^{-1}(z_i), f^{-1}(z_j))$ This distance is the weight function in the sense of Algorithm 1. We apply Algorithm 1 on the discretized domain G to obtain the discrete approximation of the length-minimizing curve $\gamma^*_{\rho_G}(a^*, b^*)$.

Table 1
Experimental results of local approximation of hyperbolic and quasihyperbolic geodesics and lengths in the unit disk. Approximated values and difference to the exact value for the hyperbolic case, are given.

h	m	$\rho^*_{\mathbb{B}^2}(p_1,p_2)$	$k^*_{\mathbb{B}^2}(p_1,p_2)$	$\epsilon_{h,m}(p_1,p_2)$	$\rho^*_{\mathbb{B}^2}(p_1,p_2)/k^*_{\mathbb{B}^2}(p_1,p_2)$
0.01	3	2.9425	2.5258	6.8054×10^{-3}	1.1623
0.01	6	2.9393	2.5230	3.6631×10^{-3}	1.1636
0.01	8	2.9405	2.5236	4.7953×10^{-3}	1.1633
0.005	3	2.9416	2.5246	5.9590×10^{-3}	1.1628
0.005	6	2.9367	2.5210	1.0694×10^{-3}	1.1645
0.005	8	2.9370	2.5211	1.3222×10^{-3}	1.1644
0.005	10	2.9370	2.5211	1.6986×10^{-3}	1.1644
0.0025	6	2.9365	2.5207	8.7360×10^{-4}	1.1647
0.0025	8	2.9362	2.5204	5.0649×10^{-4}	1.1648

3.9. Approximated quasihyperbolic geodesics. For any $a^*, b^* \in G$, the approximated quasihyperbolic geodesic $\gamma^*_{k_G}(a^*, b^*)$ on G is constructed via Algorithm 1 where the distance between z_i and z_j as in (2.13), and it is given by:

$$\frac{|z_i - z_j|}{\min\{d(z_i, \partial G), d(z_j, \partial G)\}}.$$

This distance is the weight function in the sense of Algorithm 1.

4. Experiments on the Poincaré unit disk and Schwarz-Christoffel mappings

4.1. The unit disk. We first apply our algorithm to approximate the quasihyperbolic metric of the unit disk $\mathbb{B}^2$ equipped with the hyperbolic metric. In this case, it is known that for all $x, y \in \mathbb{B}^2$ [17, Fig. 4.5., Remark 5.4]:

$$\rho_{\mathbb{B}^2}(x,y) \le 2k_{\mathbb{B}^2}(x,y) \le 2\rho_{\mathbb{B}^2}(x,y).$$

The hyperbolic geodesics will be the sub-arcs of circular arcs orthogonal to the boundary of $\mathbb{B}^2$, joining the points x and y.

Our aim is to design an experiment to show the convergence of Algorithm 1 on $\mathbb{B}^2$ with decreasing h and increasing m. With setting $p_1 = 0.9 + 0i$ and $p_2 = 0.495 + 0.495i$, we obtain $\rho_{\mathbb{B}^2}(p_1,p_2) \approx 2.9357$ by (2.2). Then we define $\epsilon_{h,m}(p_1,p_2) = |\rho_{\mathbb{B}^2}(p_1,p_2) - \rho^*_{\mathbb{B}^2}(p_1,p_2)|$ to obtain the error estimate between analytic results and approximated results.

In Table 1, the errors in the measured length difference between the approximate and exact values decrease as h decreases and m increases. The accuracy reaches a reasonable level of 10^{-4}. Another conclusion is that if we fix h and only increase m, the improvement in accuracy may be reverted in some cases.

4.2. Polygonal domains. Next, we consider two conformal mappings of the upper half-plane onto a polygonal domain. By the Schwarz-Christoffel formula, such mappings exist and efficient methods for finding these conformal mappings are given in [9].

In our next two examples, we will apply the idea described in Subsection 3.8 to the specific cases of polygonal domains. In these cases, the required conformal mapping can be obtained from the Schwarz-Christoffel formula. We use the toolbox of Driscoll [8] to compute the mapping. This toolbox has a very high accuracy, so its effect on the computational errors is negligible.

Our first example is a polygonal quadrilateral and in this case the formula is given in Theorem 2.25. Our second example is motivated by Kythe [23, pp. 226–227]. For this second example, let $k \in (0,1)$, $\xi_1 = 1/k, \xi_2 \in (0,1)$ and let

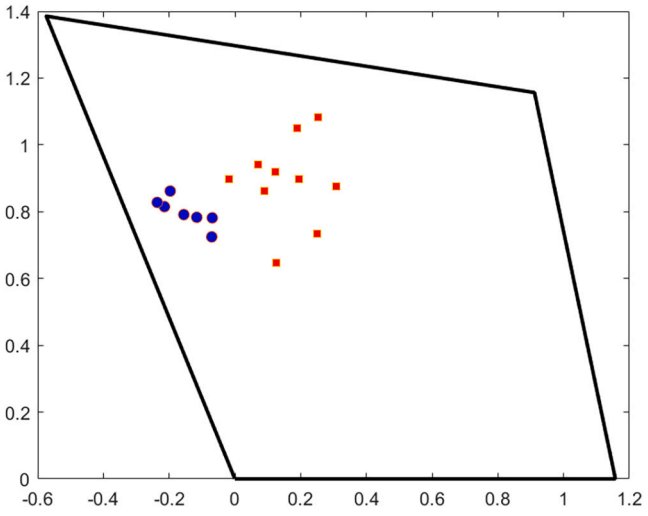

Fig. 3. The quadrilateral of Example 4.4.

$$A = -\xi_1, B = 1/k, C = 1, \text{ and } D = -\xi_2,$$

and consider the function

$$f(\zeta) = -i\zeta \int_0^1 \frac{g(\zeta,t,\xi_2)\qquad dt}{g(\zeta,t,\xi_2)g(\zeta,t,\xi_1)\sqrt{-(k^2)\zeta^2t^2+1}}, \quad g(\zeta,t,u) = \sqrt{\zeta^2t^2+u^2}. \tag{4.3}$$

This function maps the upper half-plane onto a polygon, such that the points A, B, C, D, $-D$, $-C$, $-B$, $-A$ on the real axis are mapped onto the vertices A', B', C', D', $-D'$, $-C'$, $-B'$, $-A'$ of the polygon, see Figs. 4 and 5.

4.4. Example [19]. According to Theorem 2.25, one can map the upper half-plane onto a convex polygonal quadrilateral by means of the formula (2.24) (Table 2). This transformation maps the points $0, 1, 1/r^2, \infty$ such that the points 0 and 1 are mapped on the points 0 and ${}_2F_1(a,b;c;r^2)$ of the real axis while the points $1/r^2, \infty$ are mapped into the upper half-plane. Observe the parameter constraints for the mapping (2.24):

$$0 < a, b < 1, \max\{a+b, 1\} < c \le 1 + \min\{a, b\}\,.$$

The quadrilateral illustrated in Fig. 3 is convex, with the interior angles equal to

$$b\pi, (c-b)\pi, (1-a)\pi, \text{ and } (1+a-c)\pi\,.$$

After applying Algorithm 1 locally with setting $h = 0.005, m = 4$, we obtain the results below with defining $\epsilon = |\rho_{\mathbb{H}^2}(z_1,z_2) - \rho^*_G\big(f(z_1),f(z_2)\big)|$ to describe the difference between the hyperbolic metric and the approximated hyperbolic metric.

4.5. Example, Kythe [23, pp. 226–227]. We construct a conformal map of the upper half-plane onto a given domain of Fig. 4 so that the corresponding boundary points are as in Fig. 4. We consider 10 pairs of points (z_j, w_j), $j = 1, 2, \ldots, 10$, in the upper half-plane with integer coordinates and compute their hyperbolic distance. Then we use the Kythe map h from the upper half-plane (see Fig. 5) onto the domain of Fig. 4. After applying Algorithm 1 locally with the same arguments as in the previous example, we obtain the following results, with parameter values $\xi_1 = 2.0, \xi_2 = 0.7, k = 0.8$. The results are tabulated in Table 3.

Table 2
Example 4.4.

z_1	z_2	$\rho_{\mathbb{H}^2}(z_1, z_2)$	$\rho^*_G(f(z_1), f(z_2))$	ϵ
$-2+4i$	$2i$	0.96242	0.96336	9.3957×10^{-4}
$-7+4i$	$4+2i$	2.8661	2.8697	3.6090×10^{-3}
$-6+6i$	$2+2i$	2.1459	2.1483	2.3568×10^{-3}
$-6+4i$	$2+4i$	1.7628	1.7642	1.4674×10^{-3}
$-4+4i$	$2+3i$	1.5848	1.5857	8.5910×10^{-4}
$-2+4i$	$1+2i$	1.2012	1.2038	2.6128×10^{-3}
$-2+3i$	$4+3i$	1.7628	1.7648	2.0600×10^{-3}
$-4+4i$	$2+5i$	1.2725	1.2754	2.8754×10^{-3}
$-7+4i$	$6i$	1.3751	1.3781	2.9542×10^{-3}
$-3+4i$	$1+4i$	0.96242	0.96369	1.2620×10^{-3}

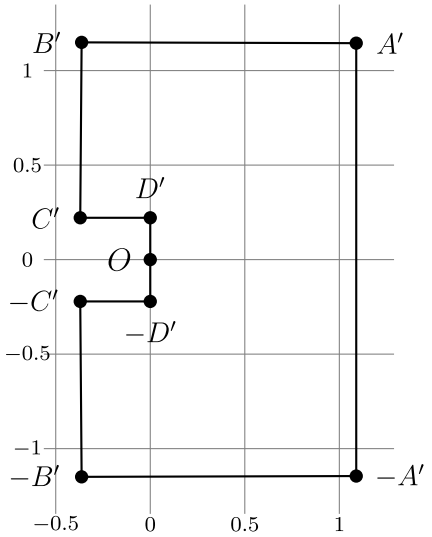

Fig. 4. This graphics shows the figure from Kythe [23, pp. 226–227]. The labels $A', B', \ldots$ indicate the image points under the mapping (4.3) of the pre-vertex points $A, B, \ldots$ on the real axis.

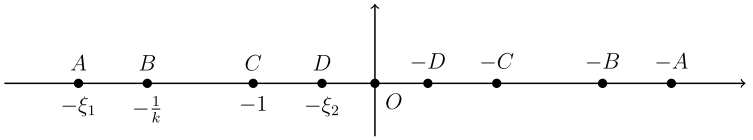

Fig. 5. This graphics reproduces the figure from Kythe [23, p. 227]. The pre-vertices $A, B, \ldots$ are on the real axis.

Table 3
Example 4.5, with $h = 0.005, m = 4$.

z_1	z_2	$\rho_{\mathbb{H}^2}(z_1, z_2)$	$\rho^*_G(f(z_1), f(z_2))$	ϵ
$-1+3i$	$4+3i$	1.5170	1.5316	1.0155×10^{-3}
$-1+4i$	$3+3i$	1.1293	1.1307	1.4684×10^{-3}
$-1+4i$	$2+2i$	1.2012	1.2025	1.2997×10^{-3}
$4i$	$2+2i$	0.96242	0.96355	1.1256×10^{-3}
$-2+4i$	$2+2i$	1.4506	1.4522	2.1042×10^{-3}
$2i$	$2+2i$	0.96242	0.96353	1.1020×10^{-3}
$-1+2i$	$3+2i$	1.7627	1.7645	1.7569×10^{-3}
$-2+4i$	$4+2i$	1.9248	1.9545	1.7300×10^{-3}

5. Bifurcation and non-uniqueness of geodesics

An interesting phenomenon arising from quasihyperbolic geometry is bifurcation of geodesics. This may arise in two specific situations:

(a) If the domain has more than one boundary component, it is possible that there are more than one quasihyperbolic geodesic between individual points choosing different routes around interior boundary components. In this case, the geodesics may go to different directions from the start, or they may have a common part and bifurcate later.
(b) It is possible that even on a simply connected domain G quasihyperbolic geodesics connecting a point x to y and one connecting it to a different point z coincide at the points of some sub-curve, and only then separate their ways.

Non-uniqueness is possible for hyperbolic geodesics in the case if the domain is multiply connected, i.e. if the domain has more than one boundary component. Note that hyperbolic geodesics joining x to separate points y, z may never have a common sub-curve. For hyperbolic domains conformally equivalent to the disk, this is easy to see, because conformal mappings are homeomorphisms, and the bifurcation property does not arise for the case of the disk, where explicit form of the geodesics is known. But the situation is very different in the case of quasihyperbolic geodesics, where bifurcation is possible already in the case of convex domains.

In this section, our goal is to experimentally demonstrate bifurcation of geodesics in several cases that are known from the literature. The examples are mostly reproductions of theoretical results from [21] and [24]. We will start with a formal definition.

5.1. Definition. Let γ_1, γ_2 be regular curves on a domain G, so that $\gamma_1, \gamma_2 : [0,1] \to G$. Suppose that there exists a point $p \in G$ s.t. $\gamma_1(t_1) = \gamma_2(t_2) = p$ for some $t_1, t_2 \in (0,1)$, the point p is a *bifurcation point* for γ_1, γ_2 if there exists $\epsilon > 0$ and a smooth strictly increasing function $\varphi : [t_1 - \epsilon, t_1 + \epsilon] \to [0,1]$ with $\varphi(t_1) = t_2$ so that either

$$\begin{cases} \gamma_1'(t) = \gamma_2'\big(\varphi(t)\big), & \text{for} \quad t \in (t_1 - \epsilon, t_1), \\ \gamma_1'(t) \neq \gamma_2'\big(\varphi(t)\big), & \text{for} \quad t \in (t_1, t_1 + \epsilon), \end{cases}$$

or

$$\begin{cases} \gamma_1'(t) \neq \gamma_2'\big(\varphi(t)\big), & \text{for} \quad t \in (t_1 - \epsilon, t_1), \\ \gamma_1'(t) = \gamma_2'\big(\varphi(t)\big), & \text{for} \quad t \in (t_1, t_1 + \epsilon). \end{cases}$$

If t_1 or t_2 is equal to 0 or 1, we may extend this definition so that only the inequality condition is required.

Based on the definition above, we design the following method to approximate the bifurcation point. It is noted that geodesics of quasihyperbolic metric are smooth, so the above definition can be applied. In the multiply connected case it is possible that geodesics between points x and y are not unique, and they may touch at individual points that are not considered as bifurcation points in the sense of this definition.

It should be noted that hyperbolic geodesics may not bifurcate on simply connected domains. This follows from the properties of hyperbolic geodesics on the unit disk combined with their conformal invariance.

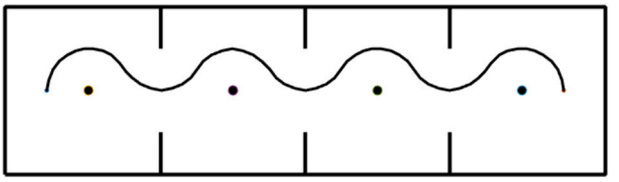

Fig. 6. Algorithm 1 on [21, Lemma 5.1], with $h = 0.025$ and $m = 4$.

Algorithm 2 Approximated Bifurcation Point Identification

Require:
$\gamma_1^* = \{z_i\}_{i=1}^m$: first path generated by Dijkstra's algorithm
$\gamma_2^* = \{w_j\}_{j=1}^n$: second path generated from Dijkstra's algorithm
$\{k_{i,\gamma_1^*} \in [-\pi, \pi] : k_{i,\gamma_1^*} = \arg(z_{i+1} - z_i), z_i \in \gamma_1^*\}_{i=1}^{m-1}$: argument sequence for γ_1^*
$\{k_{j,\gamma_2^*} \in [-\pi, \pi] : k_{j,\gamma_2^*} = \arg(w_{j+1} - w_j), w_j \in \gamma_2^*\}_{j=1}^{n-1}$: argument sequence for γ_2^*
$p \in \gamma_1^* \cup \gamma_2^*$: point satisfying $p \in [z_i, z_{i+1}]$ and $p \in [w_j, w_{j+1}]$ for some $1 \le i \le m-1, 1 \le j \le n-1$
Ensure: Approximated bifurcation point
$a \leftarrow \operatorname{argmin}_{x \in \{z_i, w_j\}} |x - p|$
$b \leftarrow \operatorname{argmin}_{x \in \{z_{i+1}, w_{j+1}\}} |x - p|$
$[a, b]$ defines the segment containing p
if $k_{i,\gamma_1^*} = k_{j,\gamma_2^*}$ **then**
  if $k_{i-1,\gamma_1^*} = k_{j-1,\gamma_2^*}$ **and** $k_{i+1,\gamma_1^*} \neq k_{j+1,\gamma_2^*}$ **then**
    return b {Case 1: approximated bifurcation point is b}
  else if $k_{i-1,\gamma_1^*} \neq k_{j-1,\gamma_2^*}$ **and** $k_{i+1,\gamma_1^*} = k_{j+1,\gamma_2^*}$ **then**
    return a {Case 2: approximated bifurcation point is a}
  end if
end if
return None {No bifurcation point found under given conditions}

5.2. Remark. Assume there exists a bifurcation point p between two smooth curves γ_1 and γ_2 defined as in Definition 5.1. When applying Algorithm 1 to obtain approximated geodesics γ_1^* and γ_2^*, and the approximated bifurcation point derived from Algorithm 2 will converge to p when refinements are done in Algorithm 1.

5.3. Domains with Punctures. An application of our method is to demonstrate numerically the results originating from the proof of [21, Lemma 5.1]. Let $G_n = R_n \setminus (P_n \cup L_n)$, where $R_n = \{a + bi \mid a \in (-1, (n-2)\sqrt{3}+1), b \in (-1, 1)\}$, $P_n = \{0, \sqrt{3}, \ldots, (n-2)\sqrt{3}\}$ and $L_n = \{a+bi \mid a \in \{\frac{\sqrt{3}}{2}, \sqrt{3}+\frac{\sqrt{3}}{2}, \ldots, (n-3)\sqrt{3}+\frac{\sqrt{3}}{2}\}, b \in (-1, -\frac{1}{2}) \cup (\frac{1}{2}, 1)\}$. Let $x = -\frac{1}{2}, y = (n-2)\sqrt{3} + \frac{1}{2}$, our aim is to approximate $\gamma_k(x, y)$ by applying Algorithm 1 on this domain.

Setting the values $h = 0.025, m = 4$, we obtain an approximation of the geodesic illustrated in Fig. 6.

Although the pictures look very similar to results in [21, Lemma 5.1], we still want to find a quantitave error estimate to compare our results to those in [21]. The following ϵ means the total error between $\{z_i\}_{i=1}^n$ and γ_1, where γ_1 defined in [21, Lemma 5.1 Proof]. If $d(z_i, \gamma_1)$ is the distance between z_i and γ_1, then we may use the error estimate from

$$\epsilon = \sum_{i=1}^{n} d(z_i, \gamma_1).$$

For the case $h = 0.025, m = 4$, the error is $\epsilon \approx 4.7577 \cdot 10^{-5}$, which shows that the points of approximated quasihyperbolic geodesic are very close to γ_1.

Based on [21, Lemma 5.1], with using the same domain G as defined in 5.3 and applying Algorithm 1 with $h = 0.025$ and $m = 4$, we obtain Fig. 7.

The theoretical bifurcation points appear at $\frac{\sqrt{3}}{2}$ and $\frac{5\sqrt{3}}{2}$ that are the same as in the proof of [21, Lemma 5.1]. Moreover, the approximated bifurcation points are 0.875 and 4.325 as the square points shown in Fig. 7, which respectively have errors 0.0089 and 0.0051.

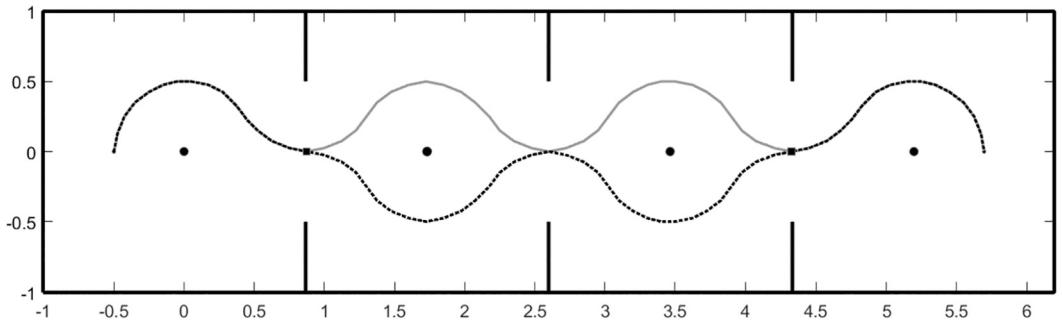

Fig. 7. Non-uniqueness of geodesics on a multiply-connected domain. In this case, the geodesic may have two or more bifurcation points depending on the taken route.

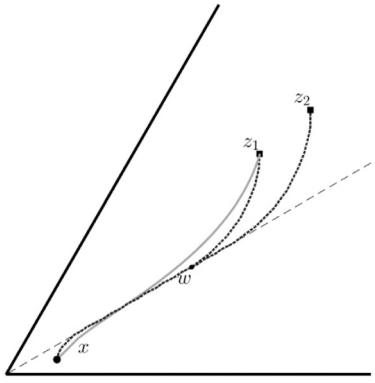

(A) Bifurcation for points on the same side of bisector.

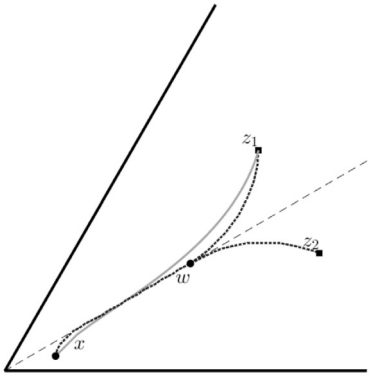

(B) Bifurcation for points on different sides of bisector.

Fig. 8. Bifurcation analysis in convex domain

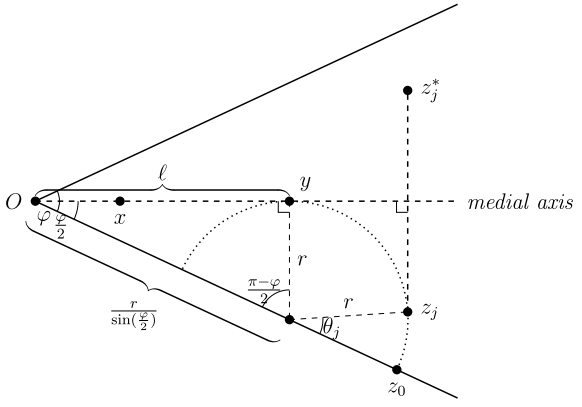

Fig. 9. The angular domain.

5.4. Convex domains. The idea of this subsection is from [24]. The aim is to demonstrate that convexity of the domain does not guarantee uniqueness of geodesics. We consider an angular domain, with the angle between the sides $\frac{\pi}{3}$, x be the start point, let w be the bifurcation point, and let z_1, z_2 be the end points, see Fig. 8.

The experiment applies Algorithm 1 locally with parameter values $h = 0.05$ and $m = 4$. The results are illustrated in Fig. 8. The solid line is the hyperbolic geodesic, and the dotted curve is the quasihyperbolic geodesic.

j	w_j	$\epsilon_{\gamma_1^*}$	$\epsilon_{\gamma_2^*}$
0	2.9	0.1049	0.1049
1	2.9	0.0342	0.0342
2	2.9	0.0276	0.0276
3	2.9	0.0304	0.0304
4	2.9	0.033	0.033
5	3.1	0.02	0.02
6	3.1	0.0245	0.0245
7	3.1	0.0071	0.0071
8	3.1	0.0042	0.0042
9	3.1	2.2204×10^{-16}	2.2204×10^{-16}

(A) The case $h = 0.025$ and $m = 8$.

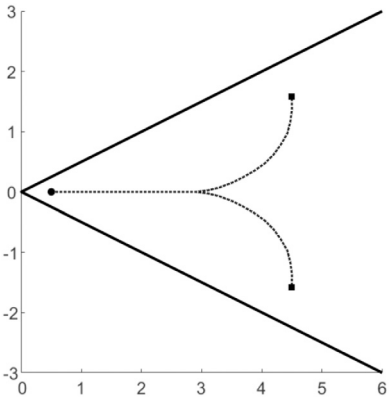

(B) The case when $j = 2$

Fig. 10. Numerical parameters and corresponding bifurcation visualization for convex domain.

We next study experimentally the ideas from [24, Theorem 4.6. Case 4]. Consider for $\varphi \in (0, \pi)$ and $L > 0$ a sequence of points in the sector $\{z : |\arg z| < \frac{\varphi}{2}, |z| < L\}$ constructed as follows

$$z_j = (\ell - ir) + re^{i(-\frac{\varphi}{2}+\theta_j)}, \quad \theta_j = \frac{j}{n} \cdot \frac{\pi + \varphi}{2}, \quad j = 1, \ldots, n$$

where $r = \ell \tan \frac{\varphi}{2}$, $0 < \ell << L$ (See Fig. 9).

For the experiment, set $L = 10^4$, $\ell = 3$, $n = 10$, and $\varphi = 2 \arctan\left(\frac{1}{2}\right)$. Also define $z_j^* := \bar{z}_j$. The point $y = \ell$ is the theoretical bifurcation point of the two geodesics joining x and z_j, x and z_j^*, respectively, when $x = \frac{1}{2}$.

Denote the approximated bifurcation points corresponding to the geodesic between x and z_j and x and z_j^*, respectively, by w_j. Our aim is to check the following:

(1) The change of w_j when increasing j from 1 to n.
(2) Whether the trace of γ_{x,z_j} and γ_{x,z_j^*} agrees with the [24, Theorem 4.6. Case 4].

Define the error estimate $\epsilon_{\gamma_1^*}$ by the formula

$$\epsilon_{\gamma_1^*} = \frac{1}{|S|} \sum_{p_j \in S} \Big| |p_j - (\ell + r \cdot i)| - r \Big|,$$

where $S = \{p_j \in \gamma_1^* \mid \mathrm{Im}\,(p_j) \neq 0\}$, and $\epsilon_{\gamma_2^*}$ is defined similarly. Both error estimates mean the average error between the theoretical quasihyperbolic geodesic and the approximated quasihyperbolic geodesic.

Applying Algorithm 1 locally with setting $h = 0.025$ and $m = 8$ and applying Algorithm 2 to get w_j, we obtain the results given in Fig. 10.

Moreover, since we cannot define points on boundary, we use $z_0 + 10^{-8}i$ to replace z_0 for the case $j = 0$. Based on the results, we conclude that the points w_j are close to y, and ϵ_{γ_1} and ϵ_{γ_2} have an error less than 10^{-2} for $1 \leq j \leq 9$.

5.5. Non-convex domains. The following example is from [21, Example 5.3]. Let G be the polygonal domain bounded by the line segments connecting the points $(-4+i, -1+i, -1+4i, 4+4i, 4-4i, -1-4i, -1-i, -4-i)$, and let $x = -2, y = -1, z_1 = i, z_2 = -i$, where we set y to be local bifurcation point and w to be approximated bifurcation point. See Fig. 11.

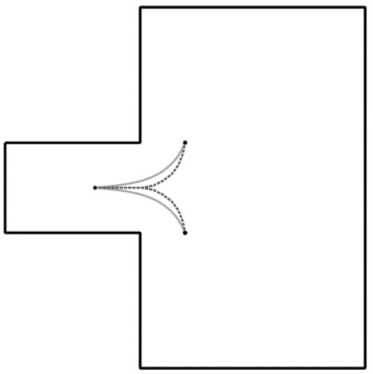

(A) Connected curves are hyperbolic geodesics on G, and dotted curves are quasihyperbolic geodesics on G.

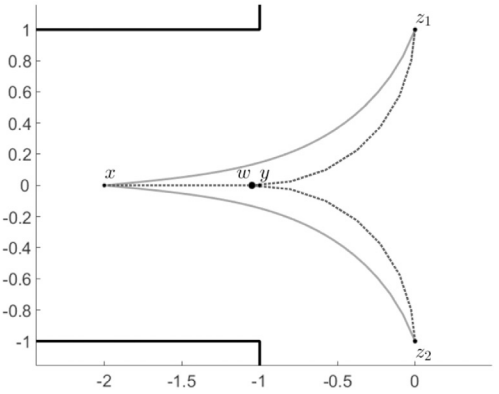

(B) Let x, y, z_1, z_2 be points described in 5.5, and curves are same as 11a described.

Fig. 11. Bifurcation analysis in non-convex domain: comparison of hyperbolic and quasihyperbolic geodesics

Table 4
Error estimates are dependent on different scales.

h	m	y	w	ϵ
0.05	2	-1	-0.8	0.2
0.05	4	-1	-0.95	0.05
0.025	2	-1	-0.8	0.2
0.025	4	-1	-0.925	0.075
0.025	8	-1	-1.05	0.05
0.02	8	-1	-1.02	0.02
0.01	2	-1	-0.76	0.24
0.01	4	-1	-0.9	0.1
0.01	8	-1	-0.96	0.04
0.01	10	-1	-1	0

In this experiment, we apply Algorithm 1 locally with several scales of refinement and apply Algorithm 2 to approximate w. Moreover, we define the error estimate as $\epsilon = |y - w|$ to describe the distance between y and w. See Table 4.

According to our experiments, when we refine the grid mesh by decreasing h and increasing m, the approximated bifurcation point w converges to y. In particular, it cannot be characterized by only considering the conformal density function.

6. Rectangular domains

Consider the quasihyperbolic geodesics joining the point pairs p_j and q_j, $j = 1, 2$, of different points. Then these two geodesics may have sub-arcs. This is closely related to the medial axis of a domain [18,24], we study the following example:

Let $G = \{a + bi \mid a \in (-3, 3), b \in (-1, 1)\}$, and consider the points $z \in G$ with $\mathrm{Re}\,(z) = -2.9$, $\mathrm{Im}\,(z) = -0.8, -0.7, \ldots, -0.1$, and $w = 2.5 - 0.5i$.

Applying Algorithm 1 with $h = 0.025, m = 8$, we obtain the results in Fig. 12.

These results show that the quasihyperbolic geodesic between z and w may have sub-arcs, which coincide with the medial axis. For some specific choices of z in this example, we see that this sub-arc is a sub-segment of the angular bisector of the rectangle.

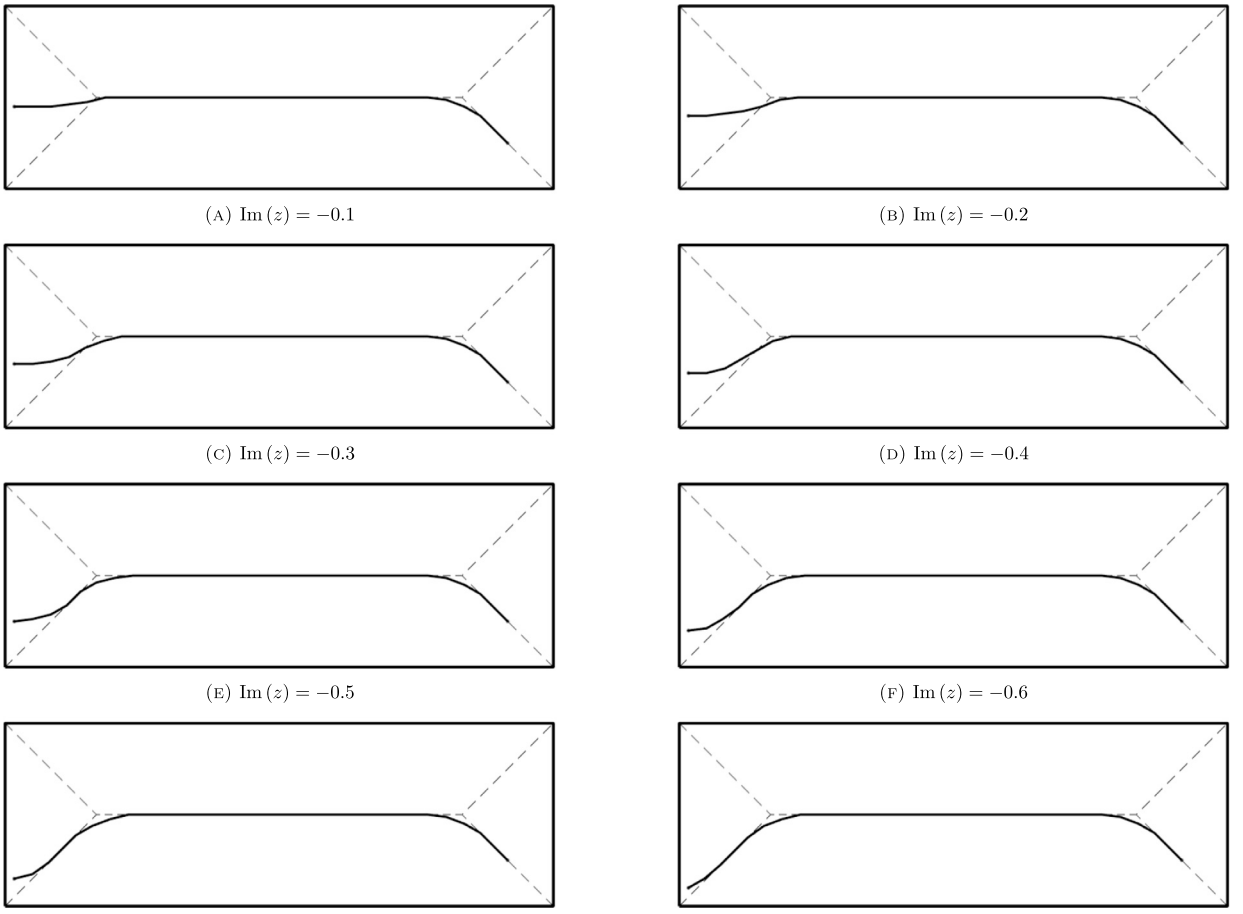

(A) $\mathrm{Im}\,(z) = -0.1$ (B) $\mathrm{Im}\,(z) = -0.2$

(C) $\mathrm{Im}\,(z) = -0.3$ (D) $\mathrm{Im}\,(z) = -0.4$

(E) $\mathrm{Im}\,(z) = -0.5$ (F) $\mathrm{Im}\,(z) = -0.6$

(G) $\mathrm{Im}\,(z) = -0.7$ (H) $\mathrm{Im}\,(z) = -0.8$

Fig. 12. Approximated quasihyperbolic geodesics in a rectangular domain.

7. Asterisk-like domains with n hands

Choose initial values $\ell_1, \ell_2, \ell_3 > 0$, and $n \in \mathbb{N}$ such that $n \geq 3$. Let $\theta = \frac{2\pi}{n}$, $\alpha = \frac{\pi}{2} - \frac{\pi}{n}$, $\beta = \frac{\pi}{n}$, $r = \frac{l_3}{\sin\beta}$, $\rho = \sqrt{\ell_1^2 + r^2 + 2\ell_1 r\cos\beta}$, $\phi = \arctan\frac{\ell_3}{r\cos\beta + \ell_1}$. We call the polygon G with $n \geq 3$ counterclockwise vertices given by

$$\{C_1, A_1, B_1, C_2, \ldots, C_j, A_j, B_j, \ldots, B_{n-1}, C_n, A_n, B_n : 1 \leq j \leq n\}$$

with $A_j = \rho \cdot e^{i(\phi + j\theta)}, B_j = r \cdot e^{i(\beta + j\theta)}, C_j = \rho \cdot e^{i(-\phi + j\theta)}$, an n-Asterisk. The case $n = 3$ is illustrated in Fig. 13.

Let $(p_1, p_2, \ldots, p_n, p_1)$ be points to be connected with hyperbolic geodesics and quasihyperbolic geodesics, where $p_j = (\mathrm{Re}\,(A_1) - \ell_2) \cdot e^{j\theta}$.

Our aim is to find the inscribed circle of hyperbolic polygon $D_\rho = \{\gamma_\rho(p_j, p_{j+1})\}$ and quasihyperbolic polygon $D_k = \{\gamma_k(p_j, p_{j+1})\}$, comparing their radius, and to observe their geometry. In our experiment, the radii of their inscribed circles are calculated from the formulas:

$$\begin{cases} r_\rho &= \min_{1\leq j\leq n}\{\min\{|z_k| : z_k \in \gamma_j\}\}, \quad \gamma_j = \gamma_\rho(p_j, p_{j+1}), \\ r_k &= \min_{1\leq j\leq n}\{\min\{|z_k| : z_k \in \gamma_j\}\}, \quad \gamma_j = \gamma_k(p_j, p_{j+1}). \end{cases}$$

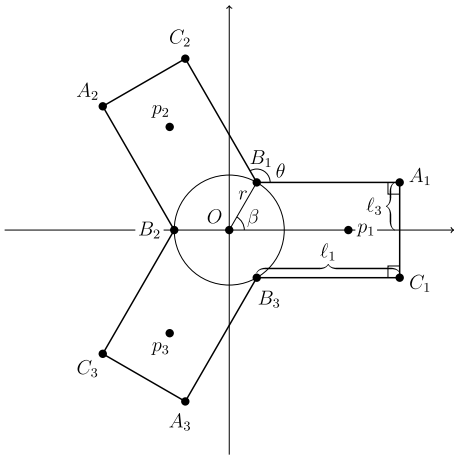

Fig. 13. A 3-asterisk.

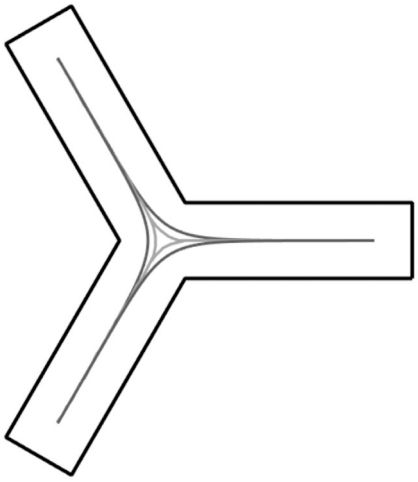

(A) The dark curve is a hyperbolic geodesic, and the light curve is a quasihyperbolic geodesic.

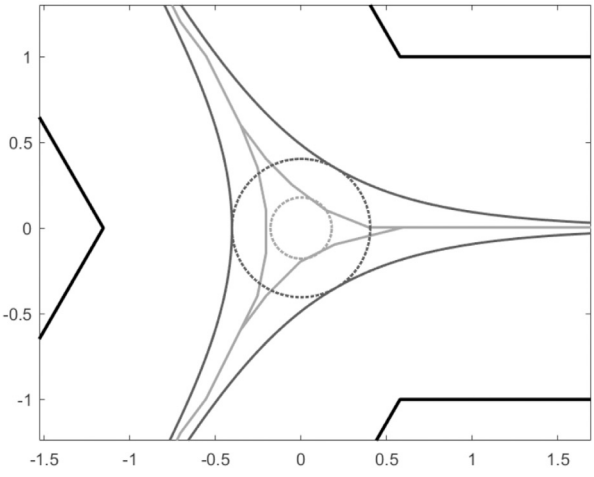

(B) The dark dotted circle is the largest inscribed circle of a hyperbolic polygon D_ρ, and the light dotted circle is the largest inscribed circle of quasihyperbolic polygon D_k.

Fig. 14. Comparison of hyperbolic and quasihyperbolic geodesics in the n-asterisk for $n = 3$.

In the experiment, we initially set $\ell_1 = 6$, $\ell_2 = \ell_3 = 1$ and apply Algorithm 1 with the parameter values $h = 0.05$ and $m = 4$. The case $n = 3$ is illustrated in Fig. 14.

We obtain the following results by changing n from 3 to 9.

Based on the above results (Table 5), we conclude that the inscribed circle of a hyperbolic polygon must contain the inscribed circle of quasihyperbolic polygon. Approximations of geodesics are illustrated in Fig. 15.

8. Remarks on Dijkstra's and A* Algorithms

Dijkstra's algorithm is a so-called *uniform cost search* algorithm, and it traverses every node of the given graph, calculates lengths of all possible paths, which makes it a low efficiency process. With respect of this question, F.C. Chrislock [6] came up with the idea of applying a *heuristic algorithm* such as A* to find shortest paths, i.e., geodesics.

The difficulty is to find the heuristic function $h(n)$, which is done just like what we do with Dijkstra's method, by applying hyperbolic or quasihyperbolic metric as our weight function. However, since we do not

Table 5
Experimental results for $\ell_1 = 6$, $\ell_2 = \ell_3 = 1$, with $h = 0.05, m = 4$.

n	$\mathrm{Re}\,(p_1)$	r	r_ρ	r_k	$\frac{r_\rho}{r_k}$
3	5.5774	1.1547	0.40365	0.17860	2.2601
4	6.0000	1.4142	0.73942	0.42426	1.7428
5	6.3764	1.7013	1.0604	0.70496	1.5042
6	6.7321	2.0000	1.3772	0.99975	1.3776
7	7.0765	2.3048	1.6928	1.3060	1.2962
8	7.4142	2.6131	2.0081	1.6169	1.2420
9	7.7475	2.9238	2.3235	1.9082	1.2176

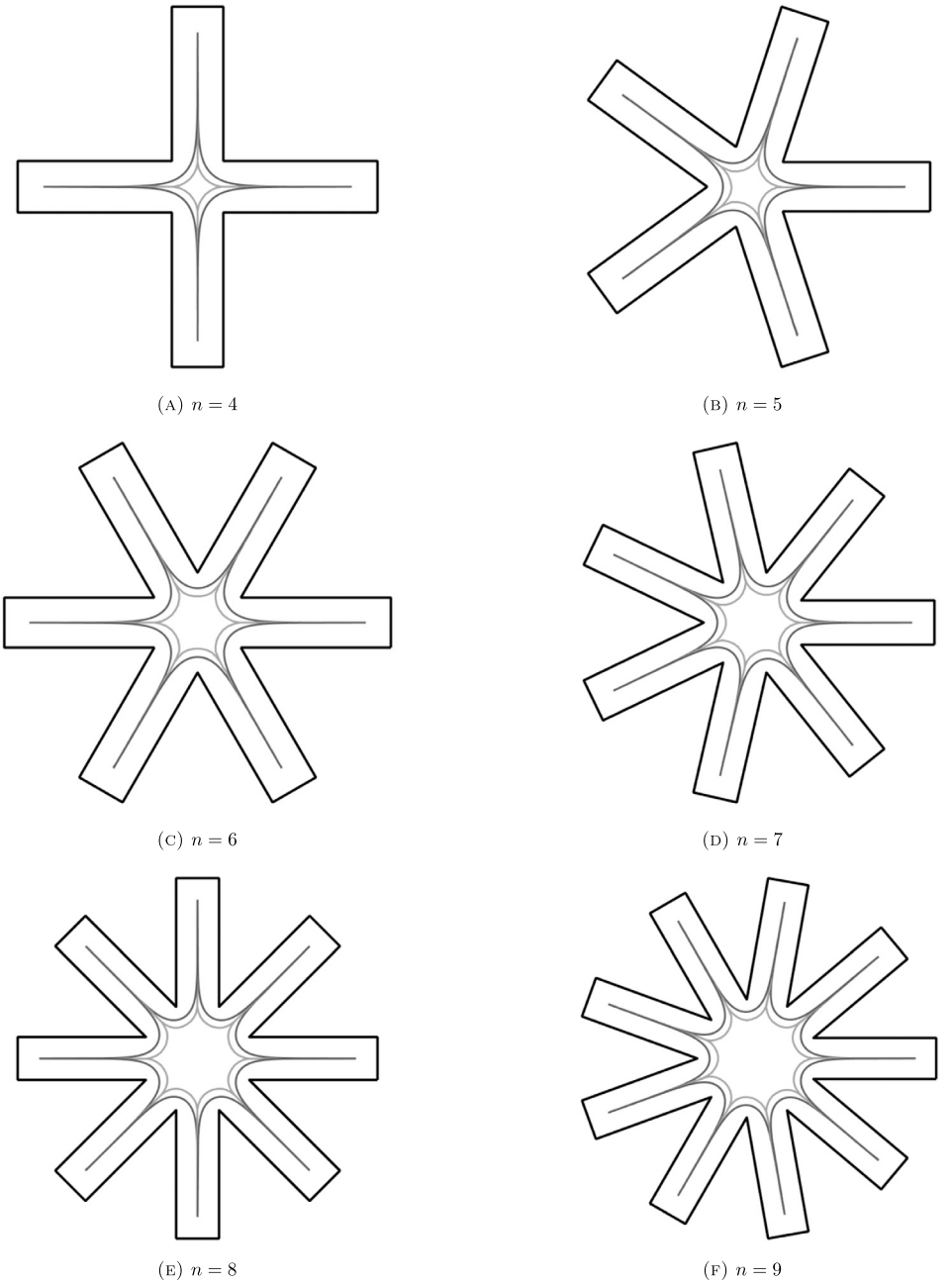

(A) $n = 4$ (B) $n = 5$

(C) $n = 6$ (D) $n = 7$

(E) $n = 8$ (F) $n = 9$

Fig. 15. Hyperbolic and quasihyperbolic polygons in n-asterisks.

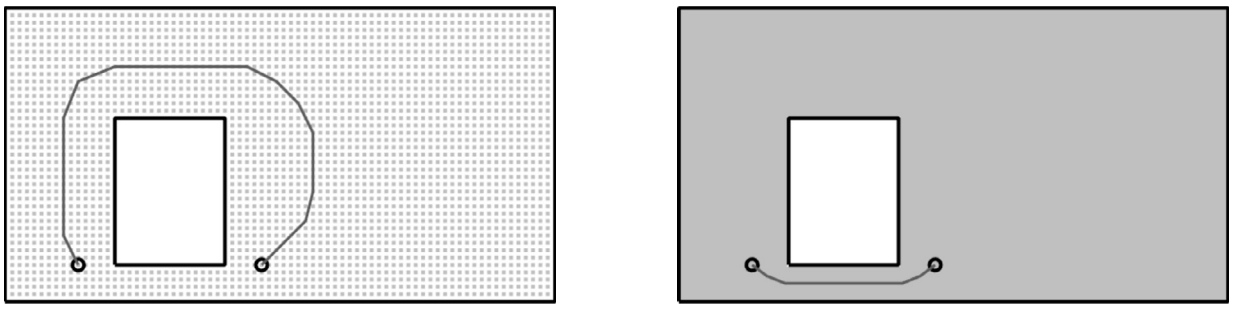

(A) $h_1 = 0.2$ (B) $h_2 = 0.1$

Fig. 16. Approximated quasihyperbolic geodesics with different h.

know the explicit formula for the quasihyperbolic metric, it is not possible to construct such a mesh with quasihyperbolically uniform discretization step h. It seems that Chrislock was also aware of this phenomenon, so he avoided searching for a formula and mapped the conflict region conformally onto to a disk instead of using the Euclidean distance as heuristic function.

One possible approach is to apply Algorithm 1 to obtain a curve first, then apply A* around a neighborhood of the curve to refine the results. This reduces the size of the graph significantly and therefore accelerates the computation. However, when designing the experiments, we considered the following case:

Let $G = R \setminus P$, where $R = \{a + bi \mid a \in [0, 15], b \in [0, 8]\}$ and $P = \{a + bi \mid a \in [3, 6], b \in [1, 5]\}$, where $p_1 = 2 + i$ and $p_2 = 7 + i$ are the points to be connected, see Fig. 16. We apply Dijkstra's method on G with different values of h and m to obtain the approximation of a quasihyperbolic geodesic between p_1 and p_2. When setting $m = 4$, the shapes of the geodesics are totally different with $h_1 = 0.2$ and $h_2 = 0.1$, respectively.

Moreover, $k^*_{G_{h_1,m}}(p_1, p_2) \approx 11.22949$ and $k^*_{G_{h_2,m}}(p_1, p_2) \approx 10.04478$. This example shows that refinement of the mesh may change the route taken by the approximated geodesic. Therefore, one needs to apply Dijkstra's method on G globally in order to handle the topology of multiply connected domains.

9. Conclusions

We have demonstrated that applying Algorithm 1 can be used to approximate quasihyperbolic geodesics on simply and multiply connected domains, including domains with punctures. In these cases we are able to obtain numerical results that are compatible with earlier theoretical results.

Our methods can be used to experimental study of many problems in geometric function theory, including theoretical properties of quasihyperbolic geodesics and balls, and triangles that play an important role in the question of Gromov hyperbolicity of these metrics. Moreover, these methods can be applied not only for hyperbolic and quasihyperbolic metrics, but for other weighted metrics as well, including Riemannian metrics on surfaces. Therefore we anticipate many potential applications.

Acknowledgments

S.G. and A.R. were supported by Natural Science Foundation of Guangdong Province (No. 2024A1515010467), Li Ka Shing Foundation GTIIT-STU Joint Research Grant (No. 2024LKSFG06), and GTIIT Education Foundation.

References

[1] M. Abramowitz, I.A. Stegun, Handbook of Mathematical Functions with Formulas, Graphs, and Mathematical Tables, Dover, 1965.
[2] G.E. Andrews, R. Askey, R. Roy, Special Functions, vol. 71, Cambridge University Press, 1999.

[3] A.F. Beardon, The Geometry of Discrete Groups, Graduate Texts in Mathematics, vol. 91, Springer, 1983.
[4] R. Bellman, On a routing problem, Q. Appl. Math. 16 (1958) 87–90.
[5] M. Bonk, J. Heinonen, P. Koskela, Uniformizing Gromov hyperbolic spaces, Astérisque (2001) viii+99.
[6] F.C. Chrislock, Pathfinding through conformal mapping, Master's thesis, NTNU, 2019.
[7] E.W. Dijkstra, A note on two problems in connexion with graphs, Numer. Math. 1 (1959) 269–271.
[8] T.A. Driscoll, Schwarz–Christoffel Toolbox for MATLAB.
[9] T.A. Driscoll, L.N. Trefethen, Schwarz-Christoffel Mapping, Cambridge University Press, Cambridge, 2002.
[10] R. Duan, J. Mao, X. Mao, X. Shu, L. Yin, Breaking the sorting barrier for directed single-source shortest paths, arXiv: 2504.17033, 2025.
[11] L.R. Ford, Network Flow Theory, Technical Report P-923, RAND Corporation, Santa Monica, CA, 1956.
[12] M.L. Fredman, R.E. Tarjan, Fibonacci heaps and their uses in improved network optimization algorithms, J. ACM 34 (1987) 596–615.
[13] F.W. Gehring, K. Hag, The Ubiquitous Quasidisk. With Contributions by Broch, Ole Jacob, Mathematical Surveys and Monographs, vol. 184, American Mathematical Soc., 2012.
[14] F.W. Gehring, G.J. Martin, B.P. Palka, An Introduction to the Theory of Higher-Dimensional Quasiconformal Mappings, Mathematical Surveys and Monographs, vol. 216, American Mathematical Soc., 2017.
[15] F.W. Gehring, B.G. Osgood, Uniform domains and the quasi-hyperbolic metric, J. Anal. Math. 36 (1979) 50–74.
[16] F.W. Gehring, B.P. Palka, Quasiconformally homogeneous domains, J. Anal. Math. 30 (1976) 172–199.
[17] P. Hariri, R. Klén, M. Vuorinen, Conformally Invariant Metrics and Quasiconformal Mappings, Springer Monographs in Mathematics, Springer, 2020.
[18] P. Hästö, Isometries of relative metrics, in: Quasiconformal Mappings and Their Applications, Narosa (2007) 57–77.
[19] V. Heikkala, M.K. Vamanamurthy, M. Vuorinen, Generalized elliptic integrals, Comput. Methods Funct. Theory 9 (2009) 75–109.
[20] J. Heinonen, Lectures on Analysis on Metric Spaces, Universitext, Springer–Verlag, 2001.
[21] R. Klén, A. Rasila, J. Talponen, On the smoothness of quasihyperbolic balls, Ann. Acad. Sci. Fenn., Math. 42 (2017) 439–452.
[22] D. Kraus, O. Roth, Conformal metrics. Topics in modern function theory, Ramanujan Math. Soc. Lect. Notes Ser. 19 (2013) 439–452.
[23] P.K. Kythe, Handbook of Conformal Mappings and Applications, CRC Press, 2019.
[24] H. Lindén, Quasihyperbolic geodesics and uniformity in elementary domains, in: Ann. Acad. Sci. Fenn. Math. Diss., 2005, p. 50, Dissertation, University of Helsinki, Helsinki, 2005.
[25] G.J. Martin, Quasiconformal and bi-Lipschitz homeomorphisms, uniform domains and the quasihyperbolic metric, Trans. Am. Math. Soc. 292 (1985) 169–191.
[26] MathWorks, Find shortest path between two single nodes - MATLAB shortestpath, https://ww2.mathworks.cn/help/matlab/ref/graph.shortestpath.html, 2023. (Accessed 8 December 2025).
[27] M. Mocanu, Generalizations of four hyperbolic–type metrics and Gromov hyperbolicity, J. Math. Anal. Appl. 552 (2025) 129729, 17pp.
[28] E.F. Moore, The shortest path through a maze, in: Proceedings of the International Symposium on the Theory of Switching, 1959, pp. 285–292.
[29] M. Nasser, M. Vuorinen, On computation of capacities and conformal invariants, J. Math. Sci. (2026), https://doi.org/10.1007/s10958-025-08141-0, arXiv:2507.11648.
[30] A. Rasila, J. Talponen, On quasihyperbolic geodesics in Banach spaces, Ann. Acad. Sci. Fenn., Math. 39 (2014) 163–173.
[31] J. Väisälä, The free quasiworld. Freely quasiconformal and related maps in Banach spaces, Banach Cent. Publ. 48 (1999) 55–118.
[32] M. Vermeer, A. Rasila, Map of the World, CRC Press, Boca Raton, FL, 2020, ©2020. An introduction to mathematical geodesy.